Received Signal Power based Sensor Zone Estimation with Maximum Likelihood Approach

Hiroki Honda*, Kazunori Hayashi†, Gurusanthosh Pabbisetty‡, and Hiroki Mori‡
* Osaka City University, Osaka, Japan
E-mail: m20tb040@zy.osaka-cu.ac.jp
† Kyoto University, Kyoto, Japan
E-mail: hayashi.kazunori.4w@kyoto-u.ac.jp
‡ Toshiba Corporation, Kawasaki, Japan
E-mail: gurusanthosh.pabbisetty@toshiba.co.jp, hiroki2.mori@toshiba.co.jp

***Abstract*—In this paper, we divide a region of interest into several zones, where a sensor node could exist in one of them, and consider the problem of estimating the zone to which it belongs. We propose a zone estimation method from the information of received signal power observed at the sensor node using maximum likelihood (ML) approach without using any distance measuring device. The estimation success probability of the proposed method is demonstrated via computer simulations. We also demonstrate the success probability of the proposed method using real data of the received power obtained through measurements.**

I. Introduction

Sensor networks collect data acquired by sensors with communication capability, and can be applied to a variety of fields such as lighting control and power monitoring [1], [2]. In particular, there is a great demand for position estimation technology using sensor networks, which has various applications such as improving operations in manufacturing and logistics, and navigation in commercial facilities. Many existing location-based services use Global Navigation Satellite System (GNSS) as a location estimation technology, but it is difficult to estimate the location in indoor environments due to the weakened signal of GNSS.

As for the location estimation in indoor environments, several methods using sensor networks have been proposed [3], [4]. Indoor position estimation methods in sensor networks can be categorized into two types: range-based approach and range-free approach. In the range-based approach, the position is estimated using the trilateration from the information of distances among nodes obtained by the distance measuring device. For example, in Active Bat [5] and Cricket [6], the distance between nodes is measured using ultrasonic waves to estimate the position. Range-based methods can generally estimate the position with high accuracy, but have the disadvantage of high cost because each node needs a device to measure the distance. On the other hand, in the range-free approach, the position of the node is estimated using the information obtained from other nodes. Range-free approach includes the Centroid method [7], the APIT method [8], and the fingerprinting approach [9]. In the Centroid method, each node obtains the location information of multiple anchor nodes, calculates its centroids, and uses the calculated value as its own estimated position. In the APIT method, each node obtains the position information of anchor nodes, and derives all triangles that can be created by combining three anchor nodes. For all possible combinations of triangles, each node verifies whether it is inside or outside the triangle, and narrows down its own possible position. However, these methods have a problem that the estimation may break down when the nodes are located at the edge of the network, because the location information of anchor nodes that can be received is limited and there may be nodes that are not located inside the triangle. In the fingerprinting approach, the received power is measured in advance at various locations in the area of interest, and results are stored in a database. The position is estimated by comparing the received power observed at the node with that in the database. However, if the surrounding environment changes after the database is created, the database needs to be constructed again.

In this paper, we consider a range-free approach that estimates the position from the received signal power observed by the sensor node without using any range measuring device. For applications such as reducing the power consumption of lighting and air conditioning systems or the survey of sojourn times in each area, fine granularity of position estimation will not be required. Instead, a coarse grained position of the node should be estimated with high probability. Thus, in this paper, we divide a region of interest into several zones, where a sensor node could exist in one of them, and consider the problem of estimating the zone to which it belongs. We propose a method to estimate the zone of the node using maximum likelihood (ML) approach based on the received signal power observed at the sensor node when known position nodes (anchor nodes) transmit radio signals multiple times. We have compared the estimation success probabilities of the proposed method, the APIT method, and the trilateration by computer simulations, and have demonstrated that the proposed method can achieve higher success rates of zone estimation than the existing methods. We have also demonstrated that zone estimation is possible with the proposed method using real data of received power obtained through measurements.

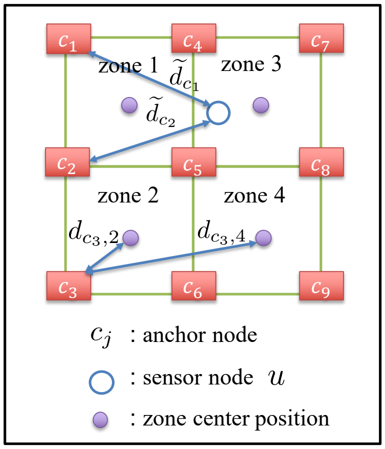

Fig. 1: Example of node placement for $Q = 9$

II. Problem Setting and Existing Methods

A. Problem Formulation

We assume that Q anchor nodes $c_1, c_2, \cdots, c_Q$ are located at predetermined known locations. Fig. 1 shows an example of the arrangement of anchor nodes when they are placed on regular grids with $Q = 9$. Assuming that a sensor node u, whose position is unknown, is placed in the area where the anchor nodes are located, we consider the problem to estimate the zone to which the sensor node u belongs from the received signal power at the sensor node u for transmissions from Q anchor nodes. Here, in the case of Fig. 1, each zone is defined as a minimum region surrounded by four anchor nodes, where the zone is denoted by $w \in \{1, 2, \cdots, R\}$ and R is the number of zones. We assume that the radio signal from the anchor node c_j includes L symbols in one transmission period, and the number of transmissions is N. Let $\widetilde{d}_{c_j}$ denote the distance between the anchor node c_j and the sensor node u, and $d_{c_j,w}$ denote the distance between the anchor node c_j and the center of zone w. The zone to which the sensor node u belongs is represented as w_u. The problem of zone estimation results in the estimation of the zone index w_u.

In the following sections, we describe received signal models at the sensor node u for two different channel models, namely, Rayleigh fading channel model and Rician fading channel model.

B. Received Signal Model of Rayleigh Fading

In this section, we assume that channels between anchor nodes and the sensor node u can be modeled as Rayleigh fading channels with path loss. The received signal at the sensor node u for the lth transmitted symbol in the nth transmission period from the anchor node c_j can be written as

$$y_{c_j}^{l,n} = h_{c_j}^{n} x_{c_j}^{l,n} + v_{c_j}^{l,n}, \tag{1}$$

where $x_{c_j}^{l,n} \in \mathbb{C}$ is the lth transmitted symbol in the nth transmission period from the anchor node c_j with mean 0 and $\left| x_{c_j}^{l,n} \right|^2 = 1$. $h_{c_j}^{n} \in \mathbb{C}$ is the channel coefficient between anchor node c_j and the sensor node u in the nth transmission period from the anchor node c_j including the impact of transmit power, and it follows a complex Gaussian distribution with mean 0 and variance $\widetilde{b}_{c_j}$ given by

$$\widetilde{b}_{c_j} = P\, \overline{r}_{\mathrm{ref}} \left(\frac{d_{\mathrm{ref}}}{\widetilde{d}_{c_j}} \right)^{\alpha}, \tag{2}$$

where α is the path loss exponent and P is the transmit power from each anchor node. We assume block fading channels, in which channel coefficients are constant during one transmission period of L symbols, but vary independently in different transmission periods. In order to take the path loss into consideration, we measure the average received power $\overline{r}_{\mathrm{ref}}$ when a signal is sent with transmit power of $P = 1$ and with inter-node distance of d_{ref}, and use the value as a reference. $v_{c_j}^{l,n} \in \mathbb{C}$ is the complex white Gaussian measurement noise with mean 0 and variance σ_{v}^2 in the received signal at the sensor node u for the lth transmitted symbol in the nth transmission period from the anchor node c_j.

For the sensor zone estimation, if we approximate the position of sensor node u to be the center of the zone w_u, the channel coefficient $h_{c_j}^{n}$ follows a complex Gaussian distribution with mean 0 and variance

$$b_{c_j,w_u} = P\, \overline{r}_{\mathrm{ref}} \left(\frac{d_{\mathrm{ref}}}{d_{c_j,w_u}} \right)^{\alpha}. \tag{3}$$

Defining the received signal vector at the sensor node u composed by L received symbols in the nth transmission period from the anchor node c_j as

$$\boldsymbol{y}_{c_j}^{n} = \left[y_{c_j}^{0,n}, y_{c_j}^{1,n}, \ \cdots \ , y_{c_j}^{L-1,n} \right]^{\mathrm{T}}, \tag{4}$$

the instantaneous total received power at the sensor node u in the nth transmission period from the anchor node c_j is given by

$$\begin{aligned} r_{c_j}^{n} &= \left(\boldsymbol{y}_{c_j}^{n} \right)^{\mathrm{H}} \boldsymbol{y}_{c_j}^{n} \\ &= L \left| h_{c_j}^{n} \right|^2 + \sum_{l=0}^{L-1} \left| v_{c_j}^{l,n} \right|^2 + \left(h_{c_j}^{n} \right)^{*} \sum_{l=0}^{L-1} \left(x_{c_j}^{l,n} \right)^{*} v_{c_j}^{l,n} \\ &\quad + h_{c_j}^{n} \sum_{l=0}^{L-1} x_{c_j}^{l,n} \left(v_{c_j}^{l,n} \right)^{*}. \end{aligned} \tag{5}$$

Here, since $x_{c_j}^{l,n}$ and $v_{c_j}^{l,n}$ are uncorrelated, we approximate as

$$\sum_{l=0}^{L-1} \left(x_{c_j}^{l,n} \right)^{*} v_{c_j}^{l,n} = 0 \tag{6}$$

and

$$\sum_{l=0}^{L-1} x_{c_j}^{l,n} \left(v_{c_j}^{l,n} \right)^{*} = 0. \tag{7}$$

Then, $r_{c_j}^{n}$ can be approximated as

$$r_{c_j}^{n} \approx L \left| h_{c_j}^{n} \right|^2 + \sum_{l=0}^{L-1} \left| v_{c_j}^{l,n} \right|^2. \tag{8}$$

C. Received Signal Model of Rician Fading

Next, we consider the case where channels between anchor nodes and the sensor node u are modeled as Rician fading channels with path loss. The received signal at the sensor node u for the lth transmitted symbol in the nth transmission period from the anchor node c_j is given by

$$y_{c_j}^{l,n} = \widetilde{h}_{c_j}^{n} x_{c_j}^{l,n} + v_{c_j}^{l,n}, \tag{9}$$

where $\widetilde{h}_{c_j}^{n} \in \mathbb{C}$ is the channel coefficient between anchor node c_j and the sensor node u in the nth transmission period from the anchor node c_j including the impact of transmit power, and it follows a complex Gaussian distribution with mean a_{c_j} and variance

$$\widetilde{g}_{c_j} = P\,\widetilde{r}_{\mathrm{ref}} \left(\frac{d_{\mathrm{ref}}}{\widetilde{d}_{c_j}} \right)^{\alpha}. \tag{10}$$

Here, $a_{c_j} \in \mathbb{C}$ is the amplitude corresponding to the line-of-sight (LoS) path between the sensor node u and the anchor node c_j. $\widetilde{r}_{\mathrm{ref}}$ represents the measured average received power of the scattered wave component when a signal is sent with transmit power of $P = 1$ and with inter-node distance d_{ref}. The Rician factor K is the ratio of the power of the LoS component to that of the scattered component and is expressed as

$$K = \frac{\left|a_{c_j}\right|^2}{\widetilde{g}_{c_j}}. \tag{11}$$

For zone estimation, if we approximate the position of sensor node u to be center of the zone w_u, the channel coefficient $\widetilde{h}_{c_j}^{n}$ follows a complex Gaussian distribution with mean a_{c_j,w_u} and variance

$$g_{c_j,w_u} = P\,\widetilde{r}_{\mathrm{ref}} \left(\frac{d_{\mathrm{ref}}}{d_{c_j,w_u}} \right)^{\alpha}, \tag{12}$$

and the Rician factor K can be written as

$$K = \frac{\left|a_{c_j,w_u}\right|^2}{g_{c_j,w_u}}. \tag{13}$$

The instantaneous total received power at the sensor node u in the nth transmission period from the anchor node c_j is given by

$$r_{c_j}^{n} \approx L \left|\widetilde{h}_{c_j}^{n}\right|^2 + \sum_{l=0}^{L-1} \left|v_{c_j}^{l,n}\right|^2 \tag{14}$$

when we approximate (6) and (7) as in the case of Rayleigh fading channel model.

D. Zone Estimation with Existing Methods

In the APIT method [8], each sensor node verifies whether it is inside or outside a triangle composed of three anchor nodes, and narrows down its own possible position. Specifically, anchor nodes transmit signals containing location information, and the sensor node obtains the position information about the anchor node's location and the received power from the anchor node. The sensor node acquires the information of multiple anchor nodes and derives all the triangles that can be created by combining the three anchor nodes. For all possible triangles, each node verifies whether it is inside or outside the triangle. The verification can be done by checking whether the distance between the sensor node and each anchor node changes shorter or longer when the sensor node moves slightly in an arbitrary direction. If the sensor node is outside the triangle, there is a direction in which the distances to all three anchor nodes get simultaneously shorter (or longer). If there is no such direction, the sensor node is inside the triangle. However, since it is difficult to move a sensor node in all directions, the APIT method considers the positions of neighboring anchor nodes of the sensor node as the positions after the movement. The distance comparison can be performed by comparing the received signal power at the sensor node and at the neighboring node. The location of the sensor node is estimated by aggregating the results of this verification with the following procedure. The entire area of interest is divided into grids, and each grid is given an initial value of 0. Each time a sensor node is determined to be inside a triangle, add 1 to the grid covered by the triangle. Each time it is determined to be on the outside, subtract 1 from the grid covered by the triangle. This process is repeated for all possible triangles, and the centroid of the grid with the largest value becomes the estimated position of the sensor node. In order to apply the APIT method to zone estimation problem considered in this paper, for each zone, we calculate the sum of the values of each grid in the zone, and we consider the zone with the largest value to be the estimated zone.

On the other hand, the trilateration is a method to estimate the position of sensor nodes using the information of distance between nodes. This method is used in range-based approach to estimate the position from the information of distances among nodes obtained by the distance measuring device. However, in range-free approach, we can also employ trilateration if the distance information is available. In our problem setting, we can obtain rough information of the distance to the anchor node from the received power observed by the sensor node. The area where the sensor nodes exist is the area where the circles with the distance as the radius centered on each anchor node overlap. Thus, the centroid of the overlapping area becomes the estimated position of the sensor node. For the zone estimation, we consider the zone to which the estimated position belongs to be the estimated zone.

III. Proposed Method with Maximum Likelihood Estimation

ML estimation is an approach to estimate parameters of the probability distribution of the observed sample. In the problem considered in this paper, the instantaneous total received power is used as the sample, and the unknown parameter to be estimated is the zone to which the sensor node u belongs.

A. Maximum Likelihood Estimation in Rayleigh Fading Model

We derive the conditional probability density function of $r_{c_j}^{n}$ in (8) given the zone to which the sensor node u belongs.

Let

$$s_{c_j}^n = L \left| h_{c_j}^n \right|^2, \quad (15)$$

$$t_{c_j}^n = \sum_{l=0}^{L-1} \left| v_{c_j}^{l,n} \right|^2, \quad (16)$$

then $r_{c_j}^n$ can be written as

$$r_{c_j}^n = s_{c_j}^n + t_{c_j}^n. \quad (17)$$

Since the sum of squares of two independent Gaussian random variables follows an exponential distribution [10], the conditional probability density function of $s_{c_j}^n$ given w_u is written as

$$p(s_{c_j}^n | w_u) = \frac{1}{L\, P\, \overline{r}_{\mathrm{ref}} \left(\frac{d_{\mathrm{ref}}}{d_{c_j,w_u}} \right)^\alpha} \exp\left(- \frac{s_{c_j}^n}{L\, P\, \overline{r}_{\mathrm{ref}} \left(\frac{d_{\mathrm{ref}}}{d_{c_j,w_u}} \right)^\alpha} \right). \quad (18)$$

On the other hand, since the sum of independent exponential random variables follows the Erlang distribution [11], the probability density function of $t_{c_j}^n$ is given by

$$p(t_{c_j}^n) = \frac{\left(t_{c_j}^n\right)^{L-1}}{(L-1)! \sigma_{\mathrm{v}}^{2L}} \exp\left(- \frac{t_{c_j}^n}{\sigma_{\mathrm{v}}^2} \right). \quad (19)$$

Moreover, since the probability density function of the sum of independent random variables is a convolution of each probability density function [12], the conditional probability density function of $r_{c_j}^n$ given w_u is written as

$$\begin{aligned} p(r_{c_j}^n | w_u) &= \frac{\left(L\, P\, \overline{r}_{\mathrm{ref}} \left(\frac{d_{\mathrm{ref}}}{d_{c_j,w_u}} \right)^\alpha \right)^{L-1}}{(L-1)! \left(L\, P\, \overline{r}_{\mathrm{ref}} \left(\frac{d_{\mathrm{ref}}}{d_{c_j,w_u}} \right)^\alpha - \sigma_{\mathrm{v}}^2 \right)^L} \\ &\cdot \exp\left(- \frac{r_{c_j}^n}{L\, P\, \overline{r}_{\mathrm{ref}} \left(\frac{d_{\mathrm{ref}}}{d_{c_j,w_u}} \right)^\alpha} \right) \\ &\cdot \left\{ \Gamma(L) - \Gamma\left(L, \left(\frac{1}{\sigma_{\mathrm{v}}^2} - \frac{1}{L\, P\, \overline{r}_{\mathrm{ref}} \left(\frac{d_{\mathrm{ref}}}{d_{c_j,w_u}} \right)^\alpha} \right) r_{c_j}^n \right) \right\}, \end{aligned} \quad (20)$$

where $\Gamma(x)$ and $\Gamma(a,x)$ represent the gamma function and the incomplete gamma function, respectively, defined as

$$\Gamma(x) = \int_0^\infty t^{x-1} \mathrm{e}^{-t} dt, \quad (21)$$

$$\Gamma(a,x) = \int_x^\infty t^{a-1} \mathrm{e}^{-t} dt. \quad (22)$$

From (20), the likelihood function when the instantaneous total received power from all anchor nodes is observed at the sensor node u is given by

$$\begin{aligned} &P(r_{c_1}^n, r_{c_2}^n, \cdots, r_{c_Q}^n | w_u) \\ &= \prod_{j=1}^{Q} \left[\frac{\left(L\, P\, \overline{r}_{\mathrm{ref}} \left(\frac{d_{\mathrm{ref}}}{d_{c_j,w_u}} \right)^\alpha \right)^{L-1}}{(L-1)! \left(L\, P\, \overline{r}_{\mathrm{ref}} \left(\frac{d_{\mathrm{ref}}}{d_{c_j,w_u}} \right)^\alpha - \sigma_{\mathrm{v}}^2 \right)^L} \right. \\ &\left. \cdot \left\{ \Gamma(L) - \Gamma\left(L, \left(\frac{1}{\sigma_{\mathrm{v}}^2} - \frac{1}{L\, P\, \overline{r}_{\mathrm{ref}} \left(\frac{d_{\mathrm{ref}}}{d_{c_j,w_u}} \right)^\alpha} \right) r_{c_j}^n \right) \right\} \right] \\ &\cdot \exp\left(- \sum_{j=1}^{Q} \frac{r_{c_j}^n}{L\, P\, \overline{r}_{\mathrm{ref}} \left(\frac{d_{\mathrm{ref}}}{d_{c_j,w_u}} \right)^\alpha} \right), \end{aligned} \quad (23)$$

assuming that the instantaneous total received power at the sensor node u from different anchor nodes is independent. Thus, the ML estimate of the zone to which the sensor node u belongs is given by solving the optimization problem of

$$\begin{aligned} \widehat{w}_u &= \arg\max_{w_u} \sum_{n=1}^{N} \left[\sum_{j=1}^{Q} \left\{ \log \left| \frac{\left(L\, P\, \overline{r}_{\mathrm{ref}} \left(\frac{d_{\mathrm{ref}}}{d_{c_j,w_u}} \right)^\alpha \right)^{L-1}}{(L-1)! \left(L\, P\, \overline{r}_{\mathrm{ref}} \left(\frac{d_{\mathrm{ref}}}{d_{c_j,w_u}} \right)^\alpha - \sigma_{\mathrm{v}}^2 \right)^L} \right| \right. \right. \\ &+ \log \left| \Gamma(L) - \Gamma\left(L, \left(\frac{1}{\sigma_{\mathrm{v}}^2} - \frac{1}{L\, P\, \overline{r}_{\mathrm{ref}} \left(\frac{d_{\mathrm{ref}}}{d_{c_j,w_u}} \right)^\alpha} \right) r_{c_j}^n \right) \right| \\ &\left. \left. - \frac{r_{c_j}^n}{L\, P\, \overline{r}_{\mathrm{ref}} \left(\frac{d_{\mathrm{ref}}}{d_{c_j,w_u}} \right)^\alpha} \right\} \right], \end{aligned} \quad (24)$$

assuming that the instantaneous received power at each transmission period is independent.

B. Maximum Likelihood Estimation in Rician Fading Model

We derive the conditional probability density function of $r_{c_j}^n$ in (14) given the zone to which the sensor node u belongs. Let

$$s_{c_j}^n = L \left| \widetilde{h}_{c_j}^n \right|^2, \quad (25)$$

$$t_{c_j}^n = \sum_{l=0}^{L-1} \left| v_{c_j}^{l,n} \right|^2, \quad (26)$$

then $r_{c_j}^n$ can be written as

$$r_{c_j}^n = s_{c_j}^n + t_{c_j}^n. \quad (27)$$

The conditional probability density function of $s_{c_j}^n$ given w_u is written as

$$\begin{aligned} p(s_{c_j}^n | w_u) &= \frac{1}{L\, P\, \widetilde{r}_{\mathrm{ref}} \left(\frac{d_{\mathrm{ref}}}{d_{c_j,w_u}} \right)^\alpha} \\ &\cdot \exp\left(- \frac{\left| a_{c_j,w_u} \right|^2 + \frac{s_{c_j}^n}{L}}{P\, \widetilde{r}_{\mathrm{ref}} \left(\frac{d_{\mathrm{ref}}}{d_{c_j,w_u}} \right)^\alpha} \right) I_0\left(\frac{2 \left| a_{c_j,w_u} \right| \sqrt{\frac{s_{c_j}^n}{L}}}{P\, \widetilde{r}_{\mathrm{ref}} \left(\frac{d_{\mathrm{ref}}}{d_{c_j,w_u}} \right)^\alpha} \right), \end{aligned} \quad (28)$$

where $I_0(z)$ denotes the zero-order modified Bessel function of the first kind, defined as

$$I_0(z) = \frac{1}{2\pi} \int_0^{2\pi} \exp\left(z \cos\theta \right) d\theta. \quad (29)$$

On the other hand, the probability density function of $t_{c_j}^n$ is given by (19). The conditional probability density function of

$r_{c_j}^n$ given w_u can be obtained by convolution of $p(s_{c_j}^n|w_u)$ and $p(t_{c_j}^n)$, but it is difficult to obtain it in a closed form because $p(s_{c_j}^n|w_u)$ contains a zero-order modified Bessel function of the first kind. The zero-order modified Bessel function of the first kind can be approximated by the exponential function when the Rician factor K is large, but it is still difficult to calculate the convolution even with this approximation. Therefore, we use the property that the Nakagami-Rice distribution can be approximated by the Nakagami-m distribution [13]. The probability density function of the Nakagami-m distribution is expressed as

$$p(z) = \frac{2m^m}{\Omega^m \Gamma(m)} z^{2m-1} \exp\left(-\frac{m}{\Omega} z^2\right). \tag{30}$$

Using the Nakagami-m distribution, the conditional probability density function of $s_{c_j}^n$ given w_u is written as

$$\begin{aligned} p(s_{c_j}^n|w_u) \;=\; & \frac{1}{L\,\Gamma(m_{c_j,w_u})}\left(\frac{m_{c_j,w_u}}{\Omega_{c_j,w_u}}\right)^{m_{c_j,w_u}} \\ & \cdot\left(\frac{s_{c_j}^n}{L}\right)^{m_{c_j,w_u}-1}\exp\left(-\frac{m_{c_j,w_u}\,s_{c_j}^n}{\Omega_{c_j,w_u}L}\right), \end{aligned} \tag{31}$$

where m_{c_j,w_u} and Ω_{c_j,w_u} are given by

$$m_{c_j,w_u} = \frac{\left(\left|a_{c_j,w_u}\right|^2 + P\,\bar{r}_{\mathrm{ref}}\left(\frac{d_{\mathrm{ref}}}{d_{c_j,w_u}}\right)^{\alpha}\right)^2}{P\,\widetilde{r}_{\mathrm{ref}}\left(\frac{d_{\mathrm{ref}}}{d_{c_j,w_u}}\right)^{\alpha}\left(2\left|a_{c_j,w_u}\right|^2 + P\,\widetilde{r}_{\mathrm{ref}}\left(\frac{d_{\mathrm{ref}}}{d_{c_j,w_u}}\right)^{\alpha}\right)}, \tag{32}$$

$$\Omega_{c_j,w_u} = \left|a_{c_j,w_u}\right|^2 + P\,\widetilde{r}_{\mathrm{ref}}\left(\frac{d_{\mathrm{ref}}}{d_{c_j,w_u}}\right)^{\alpha}, \tag{33}$$

respectively. Thus, the conditional probability density function of $r_{c_j}^n$ given w_u is obtained as

$$\begin{aligned} p(r_{c_j}^n|w_u) \;=\; & \frac{\Gamma(L)}{\Gamma(L+m_{c_j,w_u})}\left(\frac{m_{c_j,w_u}}{\Omega_{c_j,w_u}}\right)^{m_{c_j,w_u}}\left(\frac{1}{L}\right)^{m_{c_j,w_u}-1} \\ & \cdot\frac{1}{L!\sigma_{\mathrm{v}}^{2L}}(r_{c_j}^n)^{L+m_{c_j,w_u}-1}\exp\left(-\frac{r_{c_j}^n}{\sigma_{\mathrm{v}}^2}\right) \\ & \cdot{}_1F_1\left(m_{c_j,w_u}; L+m_{c_j,w_u}; \left(\frac{1}{\sigma_{\mathrm{v}}^2}-\frac{m_{c_j,w_u}}{L\Omega_{c_j,w_u}}\right)r_{c_j}^n\right), \end{aligned} \tag{34}$$

by the convolution of (19) and (31), where ${}_1F_1(a,b;z)$ denotes the general hypergeometric function, defined as

$${}_1F_1(a,b,z) = \frac{\Gamma(b)}{\Gamma(a)}\sum_{n=1}^{\infty}\frac{\Gamma(a+n)z^n}{\Gamma(b+n)n!}. \tag{35}$$

From (34), the likelihood function when the instantaneous total received power from all anchor nodes is observed at the sensor node u is given by

$$\begin{aligned} & P(r_{c_1}^n, r_{c_2}^n, \cdots, r_{c_Q}^n|w_u) \\ &= \prod_{j=1}^{Q}\left\{\frac{\Gamma(L)}{\Gamma(L+m_{c_j,w_u})}\left(\frac{m_{c_j,w_u}}{\Omega_{c_j,w_u}}\right)^{m_{c_j,w_u}}\left(\frac{1}{L}\right)^{m_{c_j,w_u}-1}\right. \\ & \cdot\frac{1}{L!\sigma_{\mathrm{v}}^{2L}}(r_{c_j}^n)^{L+m_{c_j,w_u}-1}\exp\left(-\frac{r_{c_j}^n}{\sigma_{\mathrm{v}}^2}\right) \\ & \left.\cdot{}_1F_1\left(m_{c_j,z}; L+m_{c_j,w_u}; \left(\frac{1}{\sigma_{\mathrm{v}}^2}-\frac{m_{c_j,w_u}}{L\Omega_{c_j,w_u}}\right)r_{c_j}^n\right)\right\}, \end{aligned} \tag{36}$$

assuming that the instantaneous total received power at the sensor node u from different anchor nodes is independent. Thus, the ML estimate of the zone to which the sensor node u belongs is given by solving the optimization problem of

$$\begin{aligned} \widehat{w}_u \;=\; & \arg\max_{w_u}\sum_{n=1}^{N}\left[\sum_{j=1}^{Q}\left\{\log\left(\frac{\Gamma(L)}{\Gamma(L+m_{c_j,w_u})}\right)\right.\right. \\ & +m_{c_j,w_u}\log\left(\frac{m_{c_j,w_u}}{\Omega_{c_j,w_u}}\right) + \left(m_{c_j,w_u}-1\right)\log\left(\frac{1}{L}\right) \\ & +\log\left(\frac{1}{L!\sigma_{\mathrm{v}}^{2L}}\right) + \left(L+m_{c_j,w_u}-1\right)\log(r_{c_j}^n) - \frac{r_{c_j}^n}{\sigma_{\mathrm{v}}^2} \\ & \left.\left.+\log\left({}_1F_1\left(m_{c_j,w_u}; L+m_{c_j,w_u}; \left(\frac{1}{\sigma_{\mathrm{v}}^2}-\frac{m_{c_j,w_u}}{L\Omega_{c_j,w_u}}\right)r_{c_j}^n\right)\right)\right\}\right], \end{aligned} \tag{37}$$

assuming that the instantaneous received power at each transmission period is independent.

IV. Simulation and Experimental results

In this section, we compare the estimation success probabilities of the proposed method, the APIT method, and the trilateration by computer simulations to demonstrate the validity of the proposed approach. We also demonstrate the success probability of the proposed method using real data of the received power.

A. Simulation Specifications

Fig. 2 shows the arrangement of the nodes used in the simulations. The anchor nodes are placed on 3×6 regular grid points on the ceiling of the three-dimensional space. The grid spacing is set to 3 [m], and the height from the ground to the ceiling is set to 3 [m]. Ten sensor nodes (I to X) are placed at a height of 0.42 [m] from the ground. Fig. 3 shows a view of the node arrangements shown in Fig. 2 from above, where each zone is defined as a minimum region surrounded by four anchor nodes. We consider three possible arrangements for each sensor node: center of the zone (blue), 0.75 [m] upward from the center (purple), and 0.75 [m] to the left (green), as shown in Fig. 3. Let p_1 denote the blue location, p_2 the purple location, and p_3 the green location. We evaluate the performance in two different channel models, namely, Rayleigh fading channel model and Rician fading channel model. The zone to which the sensor node belongs is estimated from the received signal power at the sensor node for transmission from all anchor nodes. This trial is repeated 100 times and the performance is evaluated using the average estimation success rate of the 10 locations. The path loss exponent is set to $\alpha = 2.35$. The transmit power is set so that the average signal-to-noise power ratio (SNR) when the signal is received by a node at a distance of $d_{\mathrm{ref}} = 3.34$ from the transmission node is 10 [dB] or 20 [dB]. For Rician fading channel model, the Rician factor is set to $K = 10$. We perform the zone estimation using K and α as parametes, and take the value when the success rate of the zone estimation is the highest as the estimated value of these factors.

B. Simulation Results in Rayleigh Fading Model

Figs. 4–6 show the simulation results of the estimation success rates of the proposed ML approach, the APIT method,

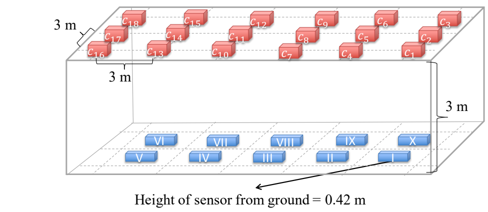

Fig. 2: Arrangement of the nodes used in the simulations

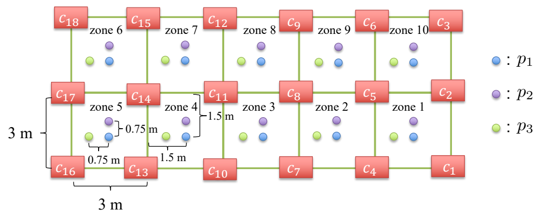

Fig. 3: Arrangment of Fig.2 as seen from above

and the trilateration assuming that the received SNR = 10 [dB], the number of transmitted symbols $L = 1, 3, 5$, and the channel between nodes can be modeled as Rayleigh fading channels, when sensor nodes are placed at p_1, p_2, and p_3, respectively. From Figs. 4–6, we can see that the proposed ML approach has a higher estimation success rate than the other methods. In the proposed ML approach, the estimation success rate increases with the increase in the number of symbols L transmitted at a time for the same number of transmissions. This is because the effect of measurement noise can be suppressed by increasing the number of transmitted symbols. In addition, the estimation success rate increases as the number of transmissions increases, and for the case where $L = 5$ and the sensor nodes are placed at p_1, the estimation success rate reaches 100% when the number of transmissions is 8 or more. This is because both the effects of fading and the effects of measurement noise can be suppressed by multiple transmissions. We can also see that the estimation success rate decreases when the sensor nodes are placed at a position deviated from the center of the zone (i.e., p_2 or p_3). This is because the node locations are approximated to the center of the zone in the proposed method. Nevertheless, for the case where $L = 5$ and the sensor nodes are placed at p_2 or p_3, the estimation success rate reaches 98% or more when the number of transmissions is 10.

Figs 7 and 8 show the estimation success rate with the proposed ML approach for each sensor node location (I to X) with the received SNR = 10 [dB] and the number of transmitted symbols $L = 5$, when sensor nodes are placed at p_1 and p_2, respectively. From Fig. 7, when the sensor nodes are placed at p_1, the ML approach does not significantly change the estimation success rate results for each node, indicating that estimation is possible regardless of the zone of the sensor nodes. On the other hand, from Fig. 8, when the nodes are placed at p_2, the success rate of the sensor nodes VI to X is

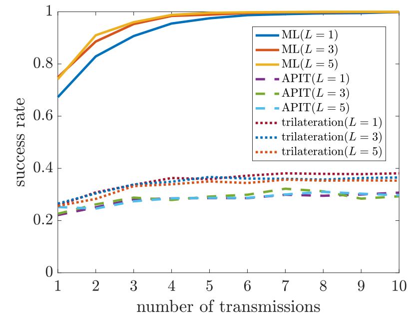

Fig. 4: Estimation success rate versus number of transmissions (Rayleigh fading, sensor node placed at p_1)

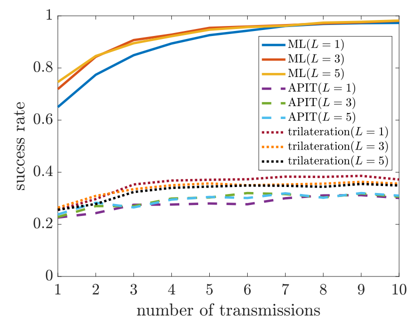

Fig. 5: Estimation success rate versus number of transmissions (Rayleigh fading, sensor node placed at p_2)

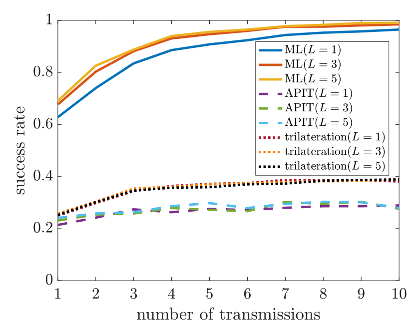

Fig. 6: Estimation success rate versus number of transmissions (Rayleigh fading, sensor node placed at p_3)

higher than that of I to V. This is because nodes I to V are more often estimated to be in zones 6 to 10 due to the upward shift in location and thus have a lower estimation success rate, while nodes VI to X are less often estimated to be in zones 1 to 5. Fig. 9 shows the estimation success rate with APIT method for each sensor node (I to X) with the received SNR = 10 [dB] and the number of transmitted symbols $L = 5$, when sensor nodes are placed at p_1. From Fig. 9, we can see that the success rate is high when the node is located in the middle of the area at III and VIII while the success rate is low for the other nodes, indicating that the estimation fails.

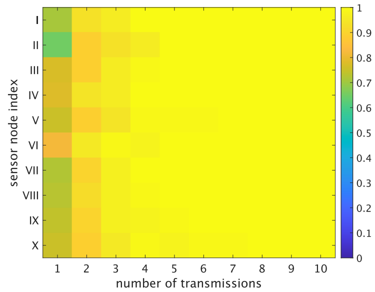

Fig. 7: Estimation success rate with proposed ML (Rayleigh fading, sensor node placed at p_1)

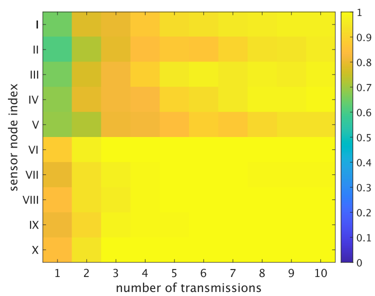

Fig. 8: Estimation success rate with proposed ML (Rayleigh fading, sensor node placed at p_2)

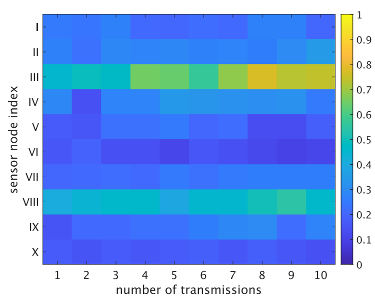

Fig. 9: Estimation success rate with APIT (Rayleigh fading, sensor node placed at p_1)

C. Simulation Results in Rician Fading Model

Figs. 10 and 11 show the simulation results of the estimation success rates of the proposed ML approach, the APIT method, and the trilateration in the Rician fading channel model with the sensor location of p_1 assuming that the received SNR = 10 [dB] and 20 [dB], respectively. From Figs. 10 and 11, we can see that as in the case of Rayleigh fading channel model, the estimation success rate of the proposed method is higher than that of other methods and the estimation success rate of the proposed method improves when the number of symbols L transmitted at a time increases for the same number of transmissions. In addition, compared to the case of Rayleigh fading channel model (Fig. 4), the estimation success rate is

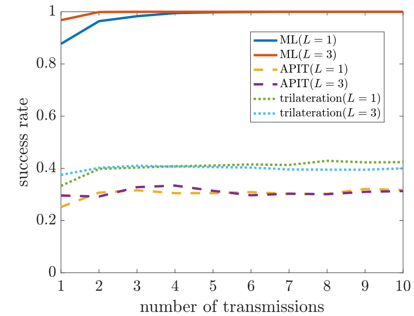

Fig. 10: Estimation success rate versus number of transmissions (Rician fading, SNR = 10 [dB])

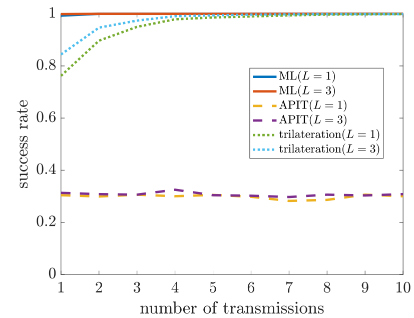

Fig. 11: Estimation success rate versus number of transmissions (Rician fading, SNR = 20 [dB])

higher in the case of Rician fading. This is because in the Rician fading channel model, the received power variation is small due to the existence of the direct wave.

D. Experiment Results

The performance of the proposed ML approach is evaluated with a simple experimental setup as shown in Fig. 12. The experiment is performed in anechoic chamber with radio wave absorbers on six sides. The arrangement of nodes is shown in Fig. 13. The anchor locations are on 3×3 regular grid points with 1.5 [m] spacing (shown in Fig. 13 as c_1 to c_9), resulting in 4 zones in the area of interest. The sensor to be located is placed at center of each zone (shown in Fig. 13 as I to IV). The target is to estimate the zone of sensor to be located using ML approach. Nordic's nRF52840 modules [14] are used as the nodes placed at the anchor locations and the sensor location. As the standard BLE (Bluetooth Low Energy) [15] uses 40 channels spaced 2 [MHz] apart, the received signal power is measured between the node at each anchor location and the sensor location in 40 BLE channels. To achieve this in a time efficient way, a multi-channel TDMA protocol named "multi-spin" (as detailed in [16]) is used. Multi-spin defines the order of transmission of sensors and synchronizes their switching on different frequency channels [16]. Multi-spin protocol is implemented on Nordic's module with 40 BLE channels

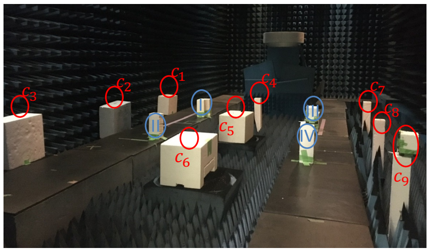

Fig. 12: Experimental setup

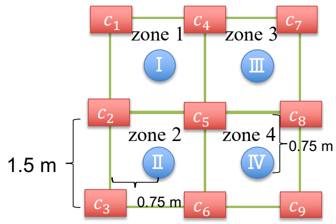

Fig. 13: Arrangement of nodes in the measurement

and accumulated received signal power among sensors. The received power measured at different frequencies corresponds to the received power at different transmission periods in the received signal model of Section II. From this, it is possible to assume that the transmission periods do not change, i.e., the channels are the same during the same frequency, and the block fading assumption is considered to be valid. Therefore, we can reasonably assume that the number of BLE channels corresponds to the number of transmissions. We measure the instantaneous received power at the sensor location, and zone estimation is performed using the instantaneous received power of 30 BLE channels, where the received power for every combination of the anchor location and the sensor location is available. We perform the zone estimation using the Rician factor, path loss exponent and SNR as parametes, and take the value when the success rate is the highest as the estimated value of these factors. Fig. 14 shows the values of likelihood in the proposed method using the measurement data with Rician fading model. From Fig. 14, we can see that zones of all four sensor nodes to be located can be estimated correctly, and the estimation success rate of 100% is achieved.

V. Conclusions

In this paper, we have proposed a method to estimate a zone of a node from the information of the received signal power using the ML approach. From the computer simulation results of the zone estimation success rate, it is found that the proposed method can achieve zone estimation within 10 transmissions from the anchor nodes in the case of both Rayleigh fading channel model and Rician fading channel model when the node is located at the center of the zone. Future work includes the performance evaluation using real data of received signal power in large-scale experimental setup. Also, it is necessary to consider a method to achieve

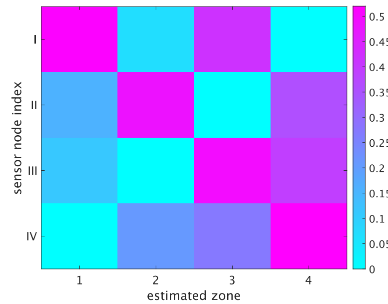

Fig. 14: Values of likelihood in the proposed method with the measurement data.

good estimation success probability even when the node is located off-center of each zone.

References

[1] Y. Yonezawa, T. Sakamoto, and Y. Ishida, "Technique to swiftly obtain information on luminaire locations after introduction of wireless lighting control systems," TOSHIBA REVIEW, vol.74, no.3, pp.44–47, May 2019.

[2] J. Yick, B. Mukherjee, and D. Ghosal, "Wireless sensor network survey," Computer networks, vol.52, no.12, pp.2292–2330, Aug. 2008.

[3] R.C. Shit, S. Sharma, D. Puthal, and A.Y. Zomaya, "Location of things (lot): A review and taxonomy of sensors localization in iot infrastructure," IEEE Communications Surveys Tutorials, vol.20, no.3, pp.2028–2061, 2018.

[4] D. Niculescu and B. Nath, "Ad hoc positioning system (aps) using aoa," IEEE INFOCOM 2003. Twenty-second Annual Joint Conference of the IEEE Computer and Communications Societies (IEEE Cat. No.03CH37428), vol.3, pp.1734–1743vol.3, 2003.

[5] M. Addlesee, R. Curwen, S. Hodges, J. Newman, P. Steggles, A. Ward, and A. Hopper, "Implementing a sentient computing system," Computer, vol.34, no.8, pp.50–56, Aug. 2001.

[6] N.B. Priyantha, A. Chakraborty, and H. Balakrishnan, "The cricket location-support system," Proceedings of the 6th Annual International Conference on Mobile Computing and Networking, pp.32–43, Assoxiation for Computing Machinery, 2000.

[7] N. Bulusu, J. Heidemann, and D. Estrin, "GPS-less low-cost outdoor localization for very small devices," IEEE Personal Communications, vol.7, no.5, pp.28–34, Oct. 2000.

[8] T. He, B.B. C. Huang, J.A. Stankovic, and T. Abdelzaher, "Range-free localization schemes for large scale sensor networks," Proceedings of the 9th Annual International Conference on Mobile Computing and Networking, pp.81–95, Association for Computing Machinery, 2003.

[9] R. Faragher and R. Harle, "Location fingerprinting with bluetooth low energy beacons," IEEE Journal on Selected Areas in Communications, vol.33, no.11, pp.2418–2428, 2015.

[10] J.G. Proakis and M. Salehi, Digital communications, 5th edition, McGraw-Hill, 2008.

[11] C. Forbes, M. Evans, N. Hastings, and B. Peacock, Statistical Distributions, 4th edition, Wiley, 2010.

[12] C.M. Grinstead and J.L. Snell, Introduction to probability, second revised edition, American Mathematical Soc., 2012.

[13] M. NAKAGAMI, "The m-distribution—a general formula of intensity distribution of rapid fading," Statistical Methods in Radio Wave Propagation, ed. by W.G. HOFFMAN, pp.3–36, Pergamon, 1960.

[14] nRF52840 Development Kit, Nordic Semiconductor, https://www.nordicsemi.com/Products/Development-hardware/nRF52840-DK, Accessed: 20th Jul, 2021.

[15] Bluetooth Wireless Technology, https://www.bluetooth.com/learn-about-bluetooth/tech-overview/, Accessed: 20th Jul, 2021.

[16] M. Bocca, O. Kaltiokallio, and N. Patwari, "Radio tomographic imaging for ambient assisted living," Evaluating AAL Systems Through Competitive Benchmarking, eds. by S. Chessa and S. Knauth, pp.108–130, Springer, Berlin, Heidelberg, 2013.